MAXIMUM POWER POINT TRACKING IN PHOTOVOLTAIC SYSTEMS USING DUAL-AXIS SOLAR TRACKER

Krishnakumar S[1], Jayasankar K C[2]

[1]Professor and Head of the Department, [2]Professor,

EEE Department, Prathyusha Engineering College, TamilNadu, India

Abstract

Improving the conversion efficiency of solar panels has become a challenging area of study for researchers. Solar trackers are an alternative to reach this goal, as has been shown in many cases, by tracking the position of the sun changes, the productivity of the panel increases. This paper presents a new design of a dual-axis solar tracker system based on a real-time measurement of solar radiation in order to improve the conversion efficiency. As a first design stage, the dynamic models for solar radiation, solar panel and electromechanical system, were obtained using Matlab-Simulink. Then a control unit for capturing the signals from radiation sensors and an inertial measurement unit, was implemented in a High-Performance 16-Bit Digital Signal Controller DSPIC33FJ202MC. The acquired data are compared with a mathematical algorithm to calculate sun's position and set the control action to orient the panel. An embedded system with real-time sampling was developed. It does not rely on external databases and takes into account the relative position between the radiation sensor and solar panel to improve the efficiency of the system. Results show an increase of 9.87% in the energy obtained with the solar tracker compared to a stati c solar panel oriented optimally. The tests were performed using two solar 200W panels operating simultaneously under the same climatic conditions.

Index Terms: Solar panel; solar radiation; dual-axis solar tracker; inertial measurement unit; digital signal processor

I. INTRODUCTION

Due to the energy crisis and environmental problems such as pollution and global warming, solar energy is becoming a very attractive solution for places with high solar density. However the cost of solar panels is still high and the conversion factor of solar energy into electrical energy is very low. Therefore, increasing energy efficiency for solar energy conversion systems, has been the focus of much research to date.

Some approaches propose to optimize the conversion efficiency of a solar panel by tracking the maximum power point (MPPT) regardless of climatic factors and the load connected to the system [1-3]. Works reported in the literature about MPPT techniques use the perturbation and observation algorithm [4], neural networks [5], fuzzy logic [6], bee colony optimization [7], adaptive control [8] and ant colony optimization [9]. Other alternative is keeping the temperature in the solar panel manufacturer's recommended value, which is generally 25°C. There are numerous researches in modeling, simulation, fabrication and implementation of thermal solar systems [10-13].

Another option is to track the sun's path in daylight hours [14]. Some researchers have conducted various studies to establish the optimal degree of tilt of a solar panel to increase the output power. Because the position of the

sun changes during the course of the day, the implementation of a solar tracker is the best solution to increase energy production.

Currently, there are two main types of solar trackers: the one axis and two axes. Studies have been developed that implement trackers of one axis [15-16], two-axis trackers with [17] and without sensors [18], and two-axis trackers using different control techniques [19-22].

In line with this research, in this paper the modeling process and implementation of a two-axis solar tracker is presented. Which has as novelty the use of a set of three radiation sensors TCS3210 consisting of arrays of photodiodes, allowing the generation of 10Hz frequency signals, which are used by the digital controller to optimize energy consumption in partially cloudy days
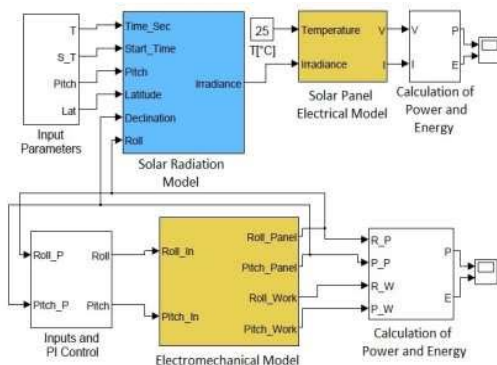
II. DYNAMIC MODEL

Fig. 1. Block diagram of the solar tracker implemented in Simulink.

Figure 1 shows the general block diagram that was implemented in Matlab-Simulink for simulation and validation of the solar tracker; which has the following subsystems: the incident solar radiation, the solar panel and the electromechanical system

2.1. Eletromechanical System Modell

The mechanical structure was manufactured based in a gear system with worm screw and a gear ratio of 1: 653, which moves the panel through the declination motor and the motor of hour angle. These motors have output torques of 14 kg-cm and 8 kg-cm respectively, that when combined with the mechanical transmission torque reaches approximately 5225 kg-cm. With this value, the torque of 540 kg-cm generated by the wind on the solar panel can be

compensated.

In Fig.2 it can be observed the solar tracker mechanical model, which has the advantage of capturing the radiation produced by the sun in azimuth and solar altitude. Thus, two automated movements are run, that allow tracking the two angles that determine the position of the sun. Therefore, the surface of the solar panels is always perpendicular to the sun every day of the year by ensuring an improvement in the efficiency of energy conversion.

Fig.2. Mechanical structure for the dual-axis solar tracker

The mechanical structure above presented and a set of DC motors constitute the electromechanical system. Two inputs Roll_in and Pitch_in were used with ranges of -12V DC to12V DC, which can control the hour angle and declination angle. The outputs used are Roll_panel and Pitch_panel and correspond to the output of the tilt sensors.

To simulate the model the SimMechanics tool was used. With this tool it was possible to model the mechanical system through rigid bodies connected by joints and thus evaluate the performance of the system before implementation. As shown in Fig.3, the first rigid object from the bottom up corresponds to the solar panel support.

The second joint corresponds to declination axis. This joint is used to move the structure and adjust it according to the value of declination calculated by the control system. The declination motor and gear system are connected through a joint actuator that takes Simulink data and converts them into SimMechanics signals. The following axis represents the hour angle axis at which a motor with torque of 14 kg-cm is connected. The last rigid body is the panel.

2.2. Declination and Hour Angle Motors

The transfer function for DC motors was experimentally found using a 12V unit step input. The values of the position and velocity were obtained using a sampling period of 15ms with a Hall Effect encoder. Based on the experimental data, the transfer function is obtained using the system identification toolbox. This one has two poles, corresponding to the poles of the electrical and mechanical part of motors. See Fig.4. With the values of the poles and the gain, the transfer function of the motors was modeled. See Eq. (1).

$$\frac{\omega(s)}{V(s)} = \frac{5571.57}{(1 + 0.37138s)(1 + 0.09175s)} \qquad (1)$$

2.3. Solar Tracking System Modelling

For the solar radiation model, the concepts of atmospheric transmittance and zenith angle depending on the time of the day were used. The zenith angle affects the amount of incident irradiation on the panel. The transmittance influences the radiation released by the clear sky depending on the zenith angle. Solar radiation is represented by Eq. (2) [23].

$$I_{ip} = I_i \, \tau \cos \theta_Z \qquad (2)$$

I_i: is the average radiation of 1000 W/m2.

θ_z: is the zenith angle in degrees. See Eq. (3).

$$\cos\theta_z = -[\cos\delta\cos\phi\cos(\theta+\alpha)+\sin\delta\sin(\theta-\alpha)] \qquad (3)$$

Where ϕ is the solar hour angle, δ is the declination angle that represents the angular position of sun with respect to the equatorial plane, θ is the geographic length in degrees and α is the tilt angle. τ is the atmospheric transmittance. See Eq. (4).

$$\tau = a + be^{-\frac{c}{\cos\theta_z}} \qquad (4)$$

Where a, b and c are radiation parameters for a horizontal surface under standard conditions.

2.4. Solar Panel Electrical Model

In Eq. (8) the solar panel mathematical model is shown [24]. With this model is only necessary to calculate the curve fitting parameter that can be obtained directly from the equation I-V. The other parameters are obtained from the electrical data of the panel.
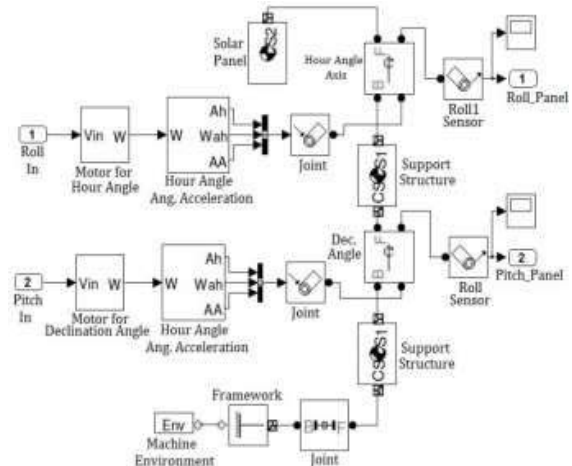

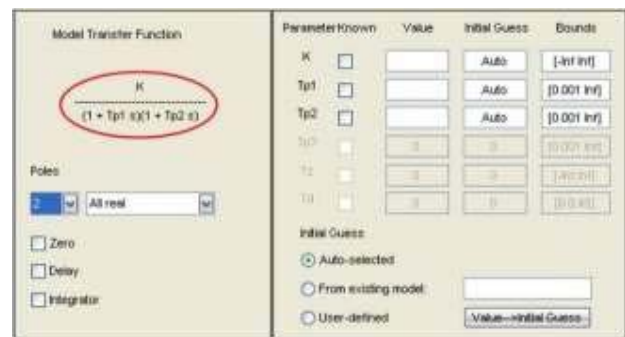**Fig. 3.** Model of the electromechanical system.

Fig. 4. Estimation of the transfer function for DC motors

In Fig.5 the radiation solar model is shown, in which the modules for calculating the zenith angle and atmospheric transmittance using a horizontal reference surface, are distinguished. The values of: solar declination, latitude, time and the roll angle of the panel, were used to calculate the zenith factor and the atmospheric transmittance.
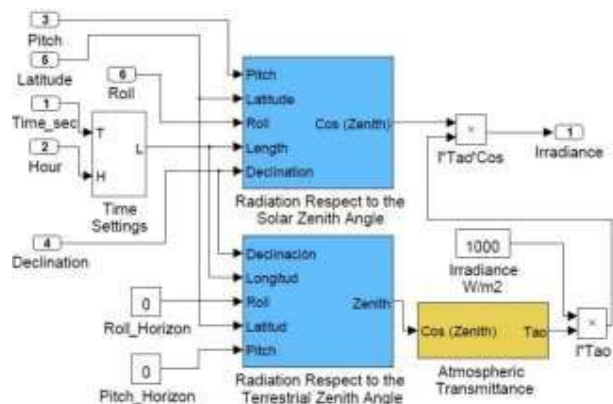

Fig. 5. Subsystem for solar radiation model.

Where V_X and I_X are the open circuit voltage and short circuit current for irradiation values and dynamic temperatures, which are defined by equations (9) and (10). b is the panel characteristic constant, it does not have units and is the unique parameter that has to be calculated.

$$I(V) = \frac{I_x}{1 - e^{\left(\frac{-1}{b}\right)}}\left[1 - e^{\left(\frac{V}{bV_x} - \frac{1}{b}\right)}\right] \qquad (8)$$

$$V_x = s\frac{E_i}{E_{in}}TC_v(T - T_n) + sV_{max}$$
$$- s(V_{max} - V_{min})e^{\left(\frac{E_i}{E_{in}}\ln\left(\frac{V_{max} - V_{oc}}{V_{max} - V_{min}}\right)\right)} \qquad (9)$$

$$I_x = p\frac{E_i}{E_{in}}[I_{sc} + TC_i(T - T_n)] \qquad (10)$$

3. Implementation of the Solar Tracker

The solar tracker consist of a digital signal processor that is responsible for processing the signals from the Inertial Measurement Unit (IMU) and the radiation sensors. The signals are compared with a mathematical algorithm that calculates the position of the sun and then performs the control action to orient the solar panel. See Fig.6.

3.1. Solar Radiation Sensor

To measure the radiation a TCS3210 sensor was used, which consists of a 4x6 matrix of silicon photodiodes that convert incident light into a frequency output. This output is directly affected by the tilt angle of the sun's rays impinging on the sensor; providing an accurate way to find the sun position during its trajectory. The frequency output delivered by the sensor is a 3.3V digital signal; allowing a direct connection to the microcontroller.

During the solar radiation measurement, the sensor was covered with a vinyl layer to prevent saturation. Thus, for a noon radiation with clear sky, the sensor generated a frequency output of 16 KHz. In addition, for a shady day, a 10Hz signal was obtained. In this way, a single sensor allows to know the position of the sun; but does not allow to define the radiation amount presented on site. For this reason, it was concluded to use an array of three sensors oriented differently on the same axis of rotation. See Fig.7.

Table 1. Electrical parameters of the 200W solar panel

Parameter	Value
Short-circuit current (I_{sc})	8.21A
Open circuit voltage (V_{oc})	32.1V
Voltage at P_{max} (V_{pmax})	26.01V
Current at P_{max} (I_{pmax})	7.69A
Temperature coefficient of voltage (T_{cv})	-0.07V/°C
Temperature coefficient of current (T_{ci})	0.002A/°C
Maximum voltage (V_{max})	33.06V
Minimum voltage (V_{min})	27.28V

3.2. Inertial Measurement Unit (IMU)

The IMU was used to measure the solar panel tilt, hence it was physically adapted to the mechanical structure of the solar tracker and their axes were aligned with the axes of the panel. The IMU used has 9 axis of data: L3GD20H 3-axis gyroscope, LSM303 3-axis compass and LSM303 3-axis accelerometer. See Fig.8.

3.3. DC Motor with Quadrature Encoder

To control the declination and hour angle, gear motors were used with stall torque of 14 kg-cm and 8 kg-cm, revolutions per minute of 350 and 150, stall current of 5A, free current of 300mA, metal internal gears, output shaft of 6mm and metal body with integrated encoder. The encoder quadrature Hall effect has a resolution of 64 pulses per revolution, therefore for a spin on the output of the gear motor 4288 pulses occur, giving a significant accuracy for any motion control application.

3.4. H-bridge Power MOSFET and Supply Source

H-bridge circuit, consisting of an array of MOSFET's, is used for controlling the movement of declination and hour angle motors. See Fig.6. For this purpose, PWM driving signals generated by the digital controller were used.
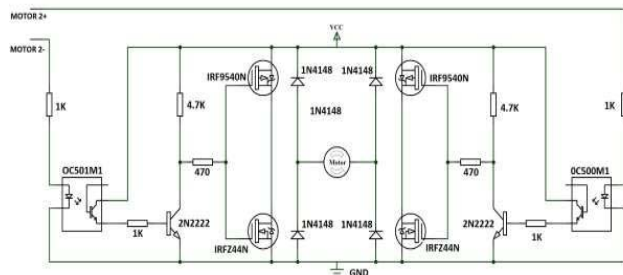

Fig. 6. H-bridge circuit diagram.

The power supply for each of the components of the solar tracker is taken directly from the solar panel. The power source consist of active elements that convert the voltage provided by the panel to different voltage ranges, which are required for the operation of each component. The circuit has output voltages of 3.3V, 5V, 12V and an additional output of 3V from a battery to power the real-time clock.

4. Results and Discussion

Once each of the stages of the prototype was implemented, the outcome is the solar tracker shown in Fig.13. Testing for different environmental conditions were made and were compared with the results of simulations.

4.1. Simulation Results

For modeling and simulation, different types of tests for each of the blocks were performed. In this document the final test that integrates all components is presented. The experiment was based on simulating the voltage, current and power generation for the dual-axis solar tracker compared to two fixed solar panels with declination angles of -9°, 0° and 23°; during the course of a day from 06:00 hours until 18:00 hours. As shown in Fig.14, the solar tracker showed better performance along the tests conducted in contrast to fixed solar panels with different declination angles.

4.2. Experimental Results

A resistive load of 10Ω was used to determine the performance of the solar tracker. Resistive loads allow an analysis of the system active power without taking into account the effects of reactive power that occur when elements such as coils and capacitors are used. Tests were performed with the solar tracker and a fixed solar panel with different declination angles. The results obtained are shown in Table 2, where N represents the day of the year and δ is the declination angle. The preliminary results show the superiority of the solar tracker compared to the energy generated by fixed solar panel. Subtracting the energy consumption of solar tracker, which varies between 6.1 and 6.5 W-h, a maximum energy increase of 9.87% was achieved taking into account different tests that were conducted in cloudy conditions.

5. Conclusions

A prototype to track the sun's path with a dual-axis solar tracker was implemented. In this way it was possible to evaluate the behavior of the system without having a finished prototype. With the simulation results, it was possible to verify that the solar tracking system allows to increase the voltage output compared with fixed solar panel systems in clear-sky conditions and in tropical areas. Tests with the prototype showed that the energy delivered by the solar tracker is greater than the energy delivered by a fixed single panel optimally oriented, including taking into account energy consumption that involves the control action of electromechanical system. Increased energy is between 5.95% and 9.87%. To ensure the rigor of testing, two solar panels of 200W from the same manufacturer were used at the same time under the same climatic conditions. A solar panel was used for the solar tracker and while the other panel was used for the fixed system.

References

[1] A. Rezaee, "Maximum power point tracking in photovoltaic (PV) systems: A review of different approaches", Renewable and Sustainable Energy Reviews. United Kingdom, vol. 65, pp. 1127-1138, November 2016.

[2] M. Saadsaoud, H. Abbassi, S. Kermiche, and M. Ouada, "Study of Partial Shading Effects on Photovoltaic Arrays with Comprehensive Simulator for Global MPPT Control", International Journal of Renewable Energy Research. Turkey, vol. 6, no. 2, pp. 413-420, 2016.

[3] M. Amine, M. Ouassaid, and M. Maaroufi, "Single-Sensor Based MPPT for Photovoltaic Systems", International Journal of Renewable Energy Research. Turkey, vol. 6, no.2, pp. 570-576, 2016.

[4] H. Bounechba, A. Bouzid, H. Snani, and A. Lashab, "Real time simulation of MPPT algorithms for PV energy system", International Journal of Electrical Power & Energy Systems. United Kingdom, vol. 83, pp. 67-78, December 2016.

[5] P. Kofinas, A. Dounis, G. Papadakis, and M.Assimakopoulos, "An Intelligent MPPT controller based on direct neural control for partially shaded PV system",

Energy and Buildings. Netherlands, vol. 90, pp. 51-64, March 2015.

[6] Y. Chen, Y Jhang, and R. Liang, "A fuzzy-logic based auto-scaling variable step-size MPPT method for PV systems", Solar Energy. United Kingdom, vol. 126, pp. 53-63,March 2016

[7] A. Benyoucef, A. Chouder, K. Kara, S. Silvestre, and O.Sahed, "Artificial bee colony based algorithm for maximum power point tracking (MPPT) for PV systems operating under partial shaded conditions", Applied Soft Computing. Netherlands, vol. 32, pp. 38-48, July 2015.

[8] R. Pradhan, and B. Subudhi, "Design and real-time implementation of a new auto-tuned adaptive MPPT control for a photovoltaic system", International Journal of Electrical Power & Energy Systems. United Kingdom, vol.64, pp. 792-803, January 2015.

[9] L. Jiang, D. Maskell, and J. Patra, "A novel ant colony optimization-based maximum power point tracking for photovoltaic systems under partially shaded conditions", Energy and Buildings. Netherlands, vol. 58, pp. 227-236, March 2013.

[10] F. Chen, and H. Yin, "Fabrication and laboratory-based performance testing of a building-integrated photovoltaic- thermal roofing panel", Applied Energy. United Kingdom, vol. 177, pp. 271-284, September 2016.

[11] C. Lamnatou, J. Mondol, D. Chemisana, and C. Maurer, "Modelling and simulation of Building-Integrated solar thermal systems: Behaviour of the coupled building/system configuration", Renewable and Sustainable Energy Reviews. United Kingdom, vol. 48, pp. 178-191, August 2015.

[12] M. Buker, and S. Riffat, "Building integrated solar thermal collectors – A review", Renewable and Sustainable Energy Reviews. United Kingdom, vol. 51, pp. 327-346, November 2015.

[13] T. Yang, and A. Athienitis, "Experimental investigation of a two-inlet air-based building integrated photovoltaic/thermal (BIPV/T) system", Applied Energy. United Kingdom, vol. 159, pp. 70-79, December 2015.

[14] J. Wu, B. Zhang, and L. Wang, "Optimum design and performance comparison of a redundantly actuated solar tracker and its nonredundant counterpart", Solar Energy. United Kingdom, vol. 127, pp. 36-47, April 2016.

[15] I. Stamatescu, I. Făgărăşan, G. Stamatescu, N. Arghira, and S. Iliescu, "Design and Implementation of a Solar- tracking Algorithm", Procedia Engineering. United Kingdom, vol. 69, pp. 500-507.

[16] R. Vieira, F. Guerra, M. Vale, and M. Araújo, "Comparative performance analysis between static solar panels and single-axis tracking system on a hot climate region near to the equator", Renewable and Sustainable Energy Reviews. United Kingdom, vol. 64, pp. 672-681, October 2016.

[17] H. Fathabadi, "Novel high efficient offline sensorless dual-axis solar tracker for using in photovoltaic systems and solar concentrators", Renewable Energy. United Kingdom, vol. 95, pp. 485-494, September 2016.

[18] V. Poulek, A. Khudysh, and M. Libra, "Self powered solar tracker for Low Concentration PV (LCPV) systems", Solar Energy. United Kingdom, vol. 127, pp. 109-112, April 2016.

[19] Y. Yao, Y. Hu, S. Gao, G. Yang, and J. Du, "A multipurpose dual-axis solar tracker with two tracking strategies", Renewable Energy. United Kingdom, vol. 72, pp. 88-98, December 2014.

[20] H. Njoku, "Upper-limit solar photovoltaic power generation: Estimates for 2-axis tracking collectors in Nigeria", Energy. United Kingdom, vol. 95, pp. 504-516, January 2016.

[21] W. Batayneh, A. Owais, and M. Nairoukh, "An intelligent fuzzy based tracking controller for a dual-axis solar PV system",

Automation in Construction. Netherlands, vol. 29, pp. 100-106, January 2013.

[22] S. Yilmaz, H. Ozcalik, O. Dogmus, F. Dincer, O. Akgol, and M. Karaaslan, "Design of two axes sun tracking controller with analytically solar radiation calculations", Renewable and Sustainable Energy Reviews. United Kingdom, vol. 43, pp. 997-1005, March 2015.

[23] Y. El Mghouchi, A. El Bouardi, Z. Choulli, and T.Ajzoul, "New model to estimate and evaluate the solar radiation", International Journal of Sustainable Built Environment. Qatar, vol. 3, pp. 225-234, December 2014.

[24] Ortiz E., "Approximation of a photovoltaic module model using fractional and integral polynomials", 38 IEEE Photovoltaic Specialists Conference, Austin, pp. 2927-2931, 3-8 June 2012.